RAYLEIGH DISK MEASUREMENTS IN PURE SUPERFLOW

Thesis by

Thomas R. Koehler

In Partial Fulfillment of the Requirements

For the Degree of

Doctor of Philosophy

California Institute of Technology

Pasadena, California

1960

ACKNOWLEDGEMENTS

The concept of the superfluid wind tunnel is due entirely to Professor John R. Pellam to whom I am indebted for encouragement and guidance throughout this investigation.

I wish to express gratitude to the Standard Oil Company of California for a fellowship 1957-1958.

ABSTRACT

The purpose of this experiment was to verify whether the superfluid component of liquid helium, flowing through a stationary normal fluid background, would exert the same torque on a Rayleigh disk as expected for perfect potential flow in classical hydrodynamics. The disk was suspended by a fine quartz fiber in a "superfluid wind tunnel" which is a device for obtaining pure superfluid flow at temperatures other than zero degrees using the fountain effect to pump helium through a chamber closed at each end by a jewelers' rouge plug. A disk 0.15 cm in radius was used with a quartz fiber of torsion constant of approximately 10^{-5} dyne-cm/deg, and the superfluid velocity was varied between 0.01 and 0.1 cm/sec. Observed torque showed the proper dependence on fluid velocity for each temperature investigated to within the experimental error of about ten percent. Also, by comparing results at different temperatures, it was possible to measure ρ_s/ρ as a function of temperature. This parameter was determined at thirteen different temperatures between 1.11°K and 2.11°K, and the results obtained agreed with previously accepted values.

TABLE OF CONTENTS

FIGURES AND TABLE

I. INTRODUCTION

A) Liquid Helium II

Many experiments have demonstrated the fact that liquid helium cooled below 2.18°K (the " λ-point") has properties exhibited by no other liquid. Among these are included the propagation of thermal waves (second sound), frictionless flow through small channels, and flow through small capillaries under a heat gradient (the fountain effect). In the temperature range above the λ-point, liquid helium is called liquid helium I and below the λ-point it is called liquid helium II.

Most of the unusual phenomena exhibited by liquid helium II can be explained in terms of the "two fluid model" first proposed by Tisza (1). Later developments by Landau (2) and Feynman (3) show that this is essentially a phenomenological model which can be derived from a more fundamental theory (Appendix 1).

The essential feature of Tisza's model is the formal division of liquid helium (liquid helium here and throughout this paper will mean liquid helium II) into two interpenetrating fluids called superfluid and normal fluid.

The superfluid component is considered to flow with no viscosity and to carry no entropy. The normal fluid component has viscosity and entropy and behaves in every way like a "classical" fluid. At every temperature there is a definite

superfluid density (ρ_s) and normal fluid density (ρ_n). The density of liquid helium itself (ρ) is practically constant and $\rho_s + \rho_n = \rho$. At the λ-point $\rho_s/\rho = 0$ and at 0^oK $\rho_n/\rho = 0$. From about 1.2^oK to the λ-point the equation $\rho_n/\rho = (T/T_\lambda)^{5.6}$ is a good representation of the behavior of the normal fluid density with temperature. (T_λ is the temperature at the λ-point).

B) Superfluid Hydrodynamics

Most of the early theoretical work in hydrodynamics was devoted to the study of the properties of a "perfect" fluid--one that has no viscosity and obeys the laws of pure potential flow. Such a fluid, of course, did not exist and no direct experimental proof of the theory was previously possible. It is natural to identify the superfluid component of liquid helium with the classical perfect fluid and to attempt to verify some of the prediction of classical hydrodynamics by experiments performed in pure superfluid flow--or superflow.

The classical theory of hydrodynamics predicts that an object immersed in a current of perfect fluid will in general feel no lift (i.e. no net force in any direction) but may feel a torque.

More specifically, if a disk of radius a is placed in a perfect fluid of density ρ moving with a uniform velocity $\vec{v}$ at infinity, the disk will feel a torque (L), tending

to turn the plane of the disk perpendicular to $\overrightarrow{v}$, of magnitude

$$L = 4/3\ a^3 \rho\ \overrightarrow{v}^{\,2} \sin 2\alpha \qquad (1)$$

where α is the angle between the normal to the disk and $\overrightarrow{v}$.

Figure 1 is a sketch of the stream lines of the flow of a perfect fluid around a disk whose normal makes an angle α with the flow direction at infinity. Points P and P' are two stagnation points. There will thus be Bernoulli forces on the disk in the direction indicated by the arrows. These forces are equal and opposite and form a couple tending to rotate the disk so as to decrease α. While the magnitude of the torque as given in equation 1 must be obtained by solving the complete hydrodynamical problem (reference 4), the above discussion indicates the reasonableness of the presence and sense of such a torque.

The fact that superfluid behaves as a perfect fluid with respect to the "zero-lift" phenomena has already been shown by Pellam and Craig (5). The present paper will present experimental evidence that superflow produces torque of a correct magnitude on a disk.

C) Previous Rayleigh-Disk Experiments

The property of a disk to respond to fluid flow was first used by Lord Rayleigh--hence the name Rayleigh disk--in his acoustical studies. In 1950 Pellam and Morse (6) used the Rayleigh disk as a detector of second sound in liquid helium.

In second sound there are two opposing velocity fields, a superfluid velocity and an oppositely directed normal fluid velocity, but there is no net mass flow. Pellam generalized the idea of Bernoulli pressure caused by a moving fluid to the two fluid (liquid helium) case with the assumption that the Bernoulli pressure at any point would be the sum of the Bernoulli pressures produced by each component acting independently.

With this assumption the disk becomes a good second sound detector. The fact that there is no net mass flow does not matter because the torque produced by each velocity field has the same sense and the two torques add. The experimental results verified the original assumption.

D) The Disk in Pure Superflow

The experiment of Pellam and Morse indicates that the Rayleigh disk would behave as expected in superflow, but is not a direct proof of this since the opposing flow of normal fluid could guide the superfluid or cause some other effect. A direct test of the behavior of the Rayleigh disk in pure superflow is thus indicated.

Liquid helium becomes pure superfluid at absolute zero. Since it is impossible to do any experiment at this temperature a means of obtaining pure superflow at higher temperatures is necessary. A device to achieve this has been proposed by Pellam (7) and has been used by Pellam and Craig (5). This device is called the "superfluid wind tunnel."

The idealized case of the superfluid wind tunnel is treated in section II and only a few sentences will be devoted to it here.

The superfluid wind tunnel is not a device that eliminates normal fluid, it is merely a device that eliminates its motion. In the wind tunnel a mass flow of liquid helium is maintained through a region in which the normal fluid is immobilized. Thus, in this region, the whole mass current is carried by the superfluid alone; or, in the tunnel, $v_s = v$ and $v_n = 0$. In this experiment a disk will be suspended from a fine quartz fiber and placed in the superfluid wind tunnel. The torque acting on the disk produced by the superflow will be determined by measuring the deflection of the disk. In practice, the performance of the disk in the superfluid wind tunnel not only verified the torque law, but also gave an independent measurement of the superfluid density (ρ_s).

II. IDEALIZED SUPERFLUID WIND TUNNEL

A) Theory

1) The Fountain Effect

The fountain effect is the name given to the fact that liquid helium will flow through very fine capillaries under a heat gradient. These fine capillaries are so small that normal fluid cannot readily penetrate them but are large enough so that superfluid can and thus are called superleaks. The operation of the wind tunnel is based on the fountain effect.

The theoretical aspects of the wind tunnel will be explained in terms of the two-fluid model of liquid helium. First consider the case of two containers of liquid helium separated by a superleak only. London (8) has shown that the two regions are in equilibrium if their Gibbs potentials are equal, which follows the general concept that the Gibbs potentials of two systems in mass-exchange equilibrium are equal.

In the liquid helium system under consideration, the two temperatures are not necessarily equal. For a small temperature difference, using pressure and temperature as variables,

$$\left(\frac{\partial g}{\partial T}\right)_p \Delta T + \left(\frac{\partial g}{\partial P}\right)_T \Delta p = 0 .$$

Substituting $\left(\frac{\partial g}{\partial T}\right)_p = -s$ (the entropy) and $\left(\frac{\partial g}{\partial p}\right)_T = 1/\rho$ the result

$$\Delta p = \rho s \Delta T \qquad (2)$$

is obtained. This is called the "London equation." The pressure differential will appear as a difference in liquid level between the two containers.

Instead of two closed containers, the system may consist of a bath of liquid helium connected through a superleak to an open tube which extends above the bath level. The same argument given before shows that a temperature difference between the tube and the bath produces a difference in fluid level.

In this case, a continuous heat supply in the tube will eventually establish a large enough temperature difference to raise the liquid level above the top of the tube. After this, the addition of more heat causes a continuous fluid flow. The name "fountain effect" comes from the fact that, if the top of the tube is drawn out and enough heat is supplied, the liquid will spurt out of the tube producing a fountain.

2) Production of Superflow

The production of pure superfluid flow utilizing the fountain effect principle is accomplished by replacing the single superleak connecting the bath to the tube with

two superleaks in series (both inside the tube). In the region between the superleaks the normal fluid is immobilized; however, superfluid is as free to flow through two superleaks as it is to flow through one so that the analysis of the fountain effect as given above still applies.

Suppose that there is a mass flow of $\dot{m}$ gms/sec through the system and further suppose that the tube has a constant area A. The fluid velocity in the region between the two superleaks where the whole mass current is carried by the superfluid alone is given by

$$v_s = \frac{\dot{m}}{\rho_s A} \tag{3}$$

while the velocity in the portion of the tube not enclosed by the two superleaks is

$$v = \frac{\dot{m}}{\rho A} \tag{4}$$

Thus, the velocity in the experimental region is enhanced with respect to the external velocity by a factor of (ρ / ρ_s).

3) Theoretical Flow Rate

The rate of flow for the wind tunnel is easily calculated for the idealized system. The physical picture shows that superfluid flows from the bath through the superleaks and into the tube. It arrives with zero entropy and must be heated to the temperature in the tube, which is essentially that of the bath. Thus, if T is the bath temperature

in degrees Kelvin, s is the entropy in joules/gm and $\dot{H}$ is the heating rate in watts. The mass flow rate is given by

$$\dot{m} = \frac{\dot{H}}{Ts} . \qquad (5)$$

Combining this with equation (3) gives the superfluid velocity as

$$v_s = \frac{\dot{H}}{S \rho_s A T} . \qquad (6)$$

In actual practice, while the essential feature of obtaining pure superflow in the region between the superleaks is achieved by the superfluid wind tunnel, the system does not quite conform to this idealized behavior. As a result, the velocity of flow must be obtained by other means than equation 6. This will be discussed in greater detail in sections III-D and IV-B.

B) Construction

A diagram indicating the construction of the idealized wind tunnel is shown in figure 2.

The two superleaks (S_1) and (S_2) are plugs of compressed jewelers rouge held in place by glass wool wads.

The position of the disk (D) and its supporting fiber (F) in the experimental region (W) is indicated. The disk would be lowered into the region from the outside through the tube (T) which must reach above the bath level (so that superfluid will not come in through it).

Region (N) encloses the heater (H) and extends above the bath level before terminating in an exhaust spout.

III. EXPERIMENTAL APPARATUS

A) Practical Superfluid Wind Tunnel

The wind tunnel as used in this experiment and some of the associated apparatus are shown in figure 3. The essential features are nearly the same as in the idealized case.

In figure 3 note that (S_1) of figure 2 has been split into two superleaks (S_1) and (S_1') and that (S_2) has been eliminated. The reason for splitting (S_1) will be explained in section IV-C. While the elimination of (S_2) was primarily to improve the optical system (see section III-E) it is clear that (S_2) is not essential for the immobilization of the normal fluid in the experimental region since there are no forces tending to move it. In practice there was no detectable difference in the performance of the wind tunnel with (S_2) or without it.

Other features that the wind tunnel of figure 3 has in common with the idealized case are the experimental region (W), the heater (H) and region (N) which encloses the heater. The area of the experimental region was 0.776 cm^2. The resistance of (H) was 56.6 ohms.

The exhaust spout (E figure 3) was modified to minimize evaporation (see section IV-B). The whole assembly was a T joint of three mm glass tubing which was held in place by a glass bulb formed over a ground glass joint (J). The

three mm tubing was extended as far as possible into N so that the surface for evaporation would be small for as great a height of N as possible. The wires for the heater were run through the three mm tubing.

The region between S_1 and S_1' was not glass but was Kovar metal. The reason for this will be explained in section IV-C.

B) Damping Assembly

As will be discussed later in section IV-D it was necessary to damp the motion of the disk. The device to do this had to meet several requirements. It had to be light weight because the fiber used was quite fine. The weight had to be distributed in such a way as to give a low enough moment of inertia so that the period would be less than about one second because it was desirable for the disk to respond rapidly to changes in the flow rate.

The type of damping that proved to be the best was magnetic damping. This was also used by Craig (5). The resistivity of copper is less by a factor of about 25,000 at liquid helium temperatures so that eddy currents are easily generated and a magnetic damping device that is useless at room temperatures can become very effective at low temperatures.

Before damping was found necessary, the disk was attached to the fiber by first gluing a small length of about 0.2 mm glass tubing (which was drawn from 3 mm tubing)

to the disk and then inserting the fiber into the other end of the tubing and gluing it in place. This was a very convenient method of mounting the disk and its essential features were retained in the final mounting assembly.

To meet the requirements of low weight and moment of inertia a small piece of copper placed near the axis of the disk and in a strong magnetic field was used (Craig (5) used a large piece of copper in a weak field).

The magnet used (M figure 3) was cylindrical with both pole pieces on the top. There was a fairly strong magnetic field along the axis of the magnet extending roughly from the level of the pole pieces to a quarter of an inch above them. There was a hole along the axis of the magnet through which the disk could be lowered.

Magnetic damping as used in this experiment provided two special problems. The first problem was that flux leaking through the bottom of the magnet exerted enough torque on the alumunized disk to hold it completely rigid. This was cured by placing the magnet in a partially hollowed cylinder of soft iron (I figure 3).

The second problem was that the magnetic field would interact with the copper used for damping which again would hold the whole assembly rigid unless the copper were mounted quite symmetrically with respect to the axis of turning. Wrapping fine wire around the glass shaft or trying to machine a small copper cylinder that would then be glued to

the shaft did not work at all. In the only method that proved satisfactory the centering of the copper used for damping and the drawing of the 0.2 mm tubing were done simultaneously by placing a piece of #20 copper wire about 0.3 inches long inside the 3 mm glass tubing, heating the tubing until the copper turned red, and then drawing the tubing out. This gave a copper bead accurately centered along the axis of a length of fine glass tubing. The disk could then be connected to the fiber as before.

Even with these precautions there was some residual interaction between the magnet and the disk assembly. The magnitude of this interaction was such that a rotation of the fibers support one degree would only turn the disk about 0.8 degrees. This was the best performance obtained after numerous trials of several different disk assemblies.

The fiber (F), the copper bead (B), the fine tubing (T) and the disk (D) are shown in figure 3. The fiber used had a torsion constant of 0.825×10^{-4} dyne-cm/degree. The radius of the disk was 0.142 cm as measured by a calibrated microscope eyepiece.

C) Angular Alignment Provisions

The fiber and disk assembly were glued to a piece of 3 mm glass tubing (R_1). This piece of tubing was kept in place in the center of the glass cylinder (O) by two cork spacers (A). (R_1) was fastened to another piece of three mm glass tubing (R_2) by epibond cement and the joint was strengthened by the copper sleeve (L).

At the top of the dewar (R_2) was fastened to a brass rod and through this to a pointer permitting measurement of rotation by means of a protractor above the dewar. This also made it possible to adjust the position of the disk to any angle with respect to the direction of fluid flow.

D) Measuring Flask

As will be explained in section IV-B, equation 6 could not be used to determine the superfluid velocity and another method had to be found. The flow rate in this experiment was too low to use pitot tubes as Craig (5) did; however, since the volume flow rate was small, the exhausting fluid could be caught in a small flask and the mass flow rate determined from the time required to fill the flask.

The flask was arranged so that it could be swung in and out under the exhaust spout and dumped when full. The position of the flask under the spout is indicated schematically in figure 3 (G) and the whole assembly is shown in figure 4.

The flask was pivoted in a wire yoke (Y figure 4). When the plunger (P) was pulled a string (S) which passed through a piece of glass tubing (T) raised the bottom of the flask (F) and dumped it. The tubing also supported the flask in space.

An O-ring seal between the plunger and the piece of brass tubing (B) in which it moved allowed free movement

but preserved vacuum tightness. (B) was also fitted with an O-ring seal so that it could turn inside a larger piece of tubing (C). This enabled the flask to be moved in and out under the spout.

The volume of the flask used was 1.9 cc.

E) Optical System

A plan view of the optical arrangement used for measuring the disk's angular position is shown in figure 5. The light source was a slide projector (P) with a vertical slit at the slide position.

The reflection of the light off the disk (D) was caught on a screen (S) placed about 80 cm away. Since the light had to pass through the dewar walls and through one wall of the wind-tunnel it became impossible to obtain a very good image on the screen. The best image obtained occupied a width on this screen equivalent to about 0.1 degree; furthermore, this would vary from place to place due to irregularities in the dewar walls.

As noted before, the forward end of the wind-tunnel was left open to simplify and improve the optical arrangement. When this was not done, the light beam had to pass through two sections of wind-tunnel walls at an angle that distorted the beam considerably.

IV. EXPERIMENTAL OPERATION

A) Introduction

In practice the wind tunnel did not perform in the idealized manner described in section II. In this section the departures from idealized behavior will be discussed and the reason for the construction of the wind tunnel as described in section III will be given. Finally, the exact experimental procedures employed will be described. It will be seen that several of the experimental procedures are necessitated by the wind tunnel's non-idealized behavior. A further discussion of some of the problems described in this section will be found in Appendix C.

B) Evaporation

The theoretical discussion of section II-A would lead one to expect that when any amount of heat was continuously supplied by the heater there would be a flow of liquid helium from the exhaust spout. This was not so in practice. It was found that a certain rate of heating $\dot{H}_o$ had to be exceeded before any flow started. Greater rates of heating would then cause a steady flow. Lesser heating rates would only cause the level in (N) to reach a certain equilibrium height above the bath level.

There is a ready explanation for this within the theoretical framework in that if the heat supplied is lost somehow rather than being used to drive the tunnel there need

be no flow. It was found that the bulk of the heat was lost by evaporation of the fluid in (N). A small amount was also lost due to imperfections in the superleaks (see section IV-C) and even less from leakage through the glass walls of (N).

In a typical operation $\dot{H}_o$ would be of the order of 0.01 watts which is a value comparable to the heating rate of about 0.025 watts used to obtain the maximum flow rates employed. Before the exhaust spout was constructed so as to minimize evaporation, H_o would be as much as 0.2 watts.

The evaporation of fluid from (N) caused an additional superfluid current through the experimental region and the effects of this will be discussed in section V-A.

An experimental test showing that most of $\dot{H}_o$ was due to evaporation was made by replacing the exhaust spout (E figure 3) with a solid plug. When this was done, a heating rate an order of magnitude less than the figure (0.01 watts) quoted for $\dot{H}_o$ would raise the fluid level up to the plug. Furthermore, after the heater was turned off, the liquid level would remain stationary for times longer than ten minutes. When the solid plug was not present the level would not remain stationary; it would return to the bath level in about five seconds.

C) Normal Fluid Leakage

Another source of heat loss, resulting from the natural difficulties encountered in the construction of superleaks,

was normal fluid leakage or heat conduction through the superleaks. Whereas ideal superleaks should permit neither normal fluid backflow nor classical heat conduction, actual devices suffer from both defects. Since these two phenomena produce the same effect experimentally, they are considered jointly simply as normal fluid leakage.

Although such normal fluid leakage was unimportant as a source of heat loss compared to evaporation, the resultant reverse normal fluid current through (W) could not be disregarded since it was large enough to produce a deflection of the disk. Fortunately, it was found possible to practically eliminate this difficulty by effectively "thermally grounding" the system to protect the region (W) from such currents.

The thermal ground is the piece of Kovar metal (K) between superleaks (S_1) and (S_1'). With this construction, any heat that is conducted through (S_1') will be grounded to the bath through the low impedance path provided by the Kovar metal rather than conducted into the region (W) through the higher impedance path (S_1'). This device essentially eliminated the leakage problem.

D) Flow Irregularities

The heat losses due to evaporation and normal fluid leakage did not seriously affect the usefulness of the wind tunnel for studying the properties of superflow; however, another and more serious complication in the wind tunnel's

performance arose which diminished the accuracy of the experiment considerably. The flow velocity in the tunnel was not constant and would change by as much as ten percent over a period of time of the order of a second.

As a result of this behavior the disk would never come to rest at any one position. Instead it would receive periodic impulses that would keep it oscillating and, furthermore, between these impulses, the disk would actually oscillate about different central positions. This indicated that the flow rate changed between the impulses.

It was originally hoped that instability was not an essential feature of superfluid flow through carborandum plug superleaks; several possible causes of erraticness were thought of and apparatus modifications were made to eliminate them. Since none of these attempts succeeded, a description of them will not be included here but will be given in Appendix C. For the present it will be assumed that unevenness of flow is an essential feature of the experiment.

An indication of the disk's motion while an angular deflection was being measured is given in figure 6. The scale at the top of the figure represents calibration marks that are placed on the screen (see section IV-E). The lines drawn down the page represent the picture that would be traced on a moving roll of film or some other recording mechanism by the light spot reflected from the

disk. The direction of increasing time is down the page. The large initial impulse given to the disk when the heater was turned on is not shown. The figure does not give actual tracings as no such were made. Instead the drawings are made from memory and are included to give some idea of the type of variations encountered.

The side-to-side motion of the disk was not caused by free oscillations but rather resulted from the disk's response to the velocity variations. When the disk swung to a new position, there was not much overshoot; this indicated adequate damping.

The average deflections shown are about 1, 4 and 6 degrees. The disturbances were of the magnitude shown for a temperature of 1.8 or 1.9 degrees. They were worse by about a factor of two at 1.4 degrees. Below 1.4 degrees, measurements were very difficult to take at all for deflections of larger than two degrees.

The stability was better than that indicated in figure 6 by about a factor of two in the vicinity of 2.1 degrees. Here it would have been possible to take measurements out to ten degrees except that at these higher temperatures the wind tunnel would saturate at a superfluid velocity corresponding to a deflection of five or six degrees and higher deflections were impossible to attain. An interesting point is that the instability was no worse after the saturation flow velocity was reached.

Along with the short term velocity variations, there was a long term drift toward lesser deflections. This is not shown in figure 6. This was due to evaporation of fluid from the whole system which lowered the bath level. According to the London equation, as the height difference between the bath and the exhaust spout increases, the temperature difference between the exhaust region and the bath also increases. This should cause an increase in the evaporation rate which would result in more heat being used to compensate for evaporative losses leaving less available to drive the wind tunnel.

Effects of the long term drift will be discussed further in sections IV-F and V-A.

Before the damping device described in section III-B was incorporated, it was practically impossible to obtain a deflection measurement with an accuracy of better than 50%. The moment of inertia of the damper increased the period of oscillation by about a factor of three so that, without it, the disk would oscillate two or three times around each central position. The amplitude of these oscillations was about equal to the average deflection; they would occasionally be larger when the impulses would come in phase with the vibrations. The combination of the motion due to the changing torque and that due to the free oscillations of the disk was more than could be followed accurately.

The damping device was quite effective in that the disk would come to rest after one or two vibrations but this did not cure the fundamental problem of the non-constancy of the flow rate. It did, however, make it possible to follow the changes in velocity by watching the various positions at which the disk momentarily came to rest.

E) Angular Calibration

A glance at the formula for torque on a disk (equation 1) will show that the torque is a maximum when $\alpha = 45^{\circ}$ so that the sin 2α term is equal to one. It can also be seen from the optical setup shown in figure 4 that when $\alpha = 45^{\circ}$ the light beam will pass through the walls of the wind tunnel in the most advantageous manner.

It was originally intended to perform the optical measurements using the null method by keeping the disk at a constant position of 45 degrees to the direction of flow at infinity and observing deflections by noting the adjustment in orientation of the pointer required to maintain this position. Two unforeseen factors prevented the use of this method. Since the deflection varied due to the flow instability, no single setting was satisfactory which made it difficult to set to an average deflection. More serious, a hysterisis effect caused by the damping mechanism would occasionally alter the position of the zero point.

The hysterisis effect was never fully explained but, unfortunately, proved impossible to eliminate. It showed up in two cases. In the first case, it was found that when the pointer was swung through a large (greater than about 15 degrees) deflection and back again to its original position the disk would not always return to its starting point but could be off by a few tenths of a degree. In the second case it was also noticed that when the disk would receive an impulse of such magnitude that it would be deflected through a large angle it would again not necessarily return to its original position. The effect was probably caused by some magnetic polarization phenomenon in the copper. The hysterisis effect was never noticed in the many different mountings that were made and used before the magnetic damping was added.

For the above mentioned reasons, the null method was not used; the angular measurements were made with the pointer kept stationary and the deflection was determined by measuring the linear displacements of the light spot on the screen (S figure 5). This method had some complications of its own but was judged to be superior to the null method.

The linear displacements of the light spot on the screen were not directly convertible to angular deflections because of two reasons. First, as has already been mentioned, despite all efforts to keep the copper bead etc.

accurately centered with respect to the axis of the fiber, there was still some residual torque on the whole assembly so that when the pointer was turned one degree, the disk would only turn about 0.8 degrees. Second, imperfections in the dewar and in the wind tunnel walls would change the direction of the light beam.

The screen was calibrated for each experiment by moving the pointer a degree at a time and marking the position of the light spot on the screen with a grease pencil. It was found experimentally that when the zero point would shift from the hysterisis effect, the other markings would shift by a similar amount so that one calibration per run was sufficient provided that the zero position was followed.

It will be shown in Appendix B that the calibration procedure is legitimate; that is, it will be shown that a torque of magnitude $\tau\Theta$ acting on the disk produces the same angular deflections as a rotation of the pointer through an angle Θ despite the presence of the perturbing torque. Of course, as a result of the perturbing torque, the angular deflection will not be equal to Θ.

The screen was calibrated after the liquid helium temperature had gone below the λ-point but before any heat was supplied by (H). After calibration, enough heat was supplied to raise the fluid level in (N) up to nearly the level of the exhaust spout. This would usually disturb the zero position and so the zero was re-set before beginning the data taking.

F) Data Recording

The data recorded were Θ and t where Θ was the angular deflection that the disk suffered when the flow rate was such as to fill the flask in a time t. After calibrating the screen, the heat input would be increased so that the liquid helium would come out of the exhaust spout at some desired rate. There would occasionally be a long term drift in the zero position of 0.1 or 0.2 degrees which was attributed to the same phenomenon that caused the hysterisis. Because of this the small deflection measurements were always taken immediately after checking the zero position so that they would be the most accurate points. For deflections of greater than about four degrees the shifts in the zero were small compared to the errors introduced by the instability in the flow.

Usually the first angular deflection measured would be in the neighborhood of one degree, then higher deflections would be measured in approximately one degree increments. At some point the instabilities would become so large that greater angular deflections were impossible to measure accurately. When this occurred, the zero position would be checked and more points taken.

The fundamental problem in obtaining accurate data was, of course, the uncertainty in the angular deflection measurements. In taking a deflection reading the motion of the light spot on the screen would be followed for a minute or

two and then a decision about the average angular deflection would be made. This decision was actually based on the behavior of the disk during the last ten or fifteen seconds; watching the movement of the disk during the time preceding this merely enabled the experimenter to develop a "feeling" for the disk's behavior.

The time required to fill the flask was measured immediately after the angular deflection measurement was made. The damping was good enough so that the transient oscillations given the disk by maneuvering the flask etc. would die out during the filling of the flask and the deflection of the disk could be noted after the timing measurement as a check. It was not possible to follow the disk's motion during much of the filling time so that the possibility of a sudden and large change of average velocity during this time was an always present source of error.

The long term drift caused by evaporation of fluid from the bath produced a noticeable effect over times of the order of five minutes; however, its effect was small compared to other experimental errors during the half a minute or so required for the determination of the disk's position and the filling of the flask.

The temperature was controlled manually by adjusting the vacuum pump valve and was usually maintained constant to within about 0.01 degrees K. The variation of ρ_s was negligible over this range even at higher temperatures.

The peculiar motion of the disk made the recording of angular deflections a somewhat subjective matter and possibly this could have introduced a certain lack of correlation observed between experiments performed on different days.

V. ANALYSIS

A) Evaporation Current Effects

The theoretical equation for the torque on a disk was given by equation 1 as

$$L = 4/3\ a^3 \rho\ v^2 \sin 2\alpha.$$

In this case, ρ becomes ρ_s and v becomes v_s, the superfluid velocity. Also, if τ is the torsion constant of the fiber and θ the deflection of the disk

$$L = \tau\ \theta. \tag{7}$$

Since v_s is measured in terms of the time required to fill a flask of volume V, the substitution

$$v_s = \frac{\rho V}{\rho_s\ At} \tag{8}$$

must be made in equation 1. All of these substitutions would give

$$\tau\theta = 4/3\ a^3 \rho \frac{V^2}{A^2} \frac{1}{t^2} \frac{1}{(\rho_s/\rho)} \tag{9}$$

with $\sin 2\alpha = 1$. The deflections observed were never greater than eight degrees so the approximation $\sin 2\alpha = 1$ is a good one and will always be used.

The expressions of equations 8 and 9 constitute an over simplification to the extent that losses resulting from evaporation are neglected in computing the superfluid traversing the experimental region. Accordingly, v_s is larger than is indicated by equation 8 since the time flow

rate also includes supplying whatever helium evaporates from the exhaust region. The more accurate expression for superfluid flow velocity then becomes

$$v_s = \frac{V}{\rho_s A t} + v_e \qquad (10)$$

where v_e represents the "effective velocity" attributed to such evaporation.

If a known amount of heat $\dot{H}_e$ is being dissipated per second by evaporation, the additional superfluid current caused by this can be calculated in the following manner: a quantity of helium $\dot{m}_e$ flows through the superleak per second, arrives with zero entropy and is raised to a temperature T which requires an amount of heat $\dot{m}_e Ts$ per second. This same quantity of liquid helium then evaporates using an additional quantity of heat $\dot{m}_e L$ per second, where L is the latent heat of evaporation. Conservation of heat gives the mass flow rate as

$$\dot{m}_e = \frac{\dot{H}_e}{L + Ts}$$

with a resulting superfluid velocity

$$v_e = \frac{\dot{H}_e}{\rho_s (L + Ts) A} \qquad (11)$$

This additional superfluid current is by no means negligible. The effects of v_e on the experimental behavior may best be illustrated in terms of a specific example. The heat of vaporization of liquid helium is in the neighborhood of

24 joules per gram. Since most of H_o is due to evaporation, the figure 0.01 watts given previously for H_o can be substituted for H_e in equation 11. Making these substitutions, a superfluid velocity of ρ/ρ_s 0.004 cm/sec results (Ts is never larger than 3.3 joules/gm and so can be ignored compared to L). This velocity, by itself, produces an angular deflection of less than 0.1 degree, which is immeasurable.

Now consider the case where the flask measurement gives a velocity value of 0.05 cm/sec. The true value then becomes 0.054 cm/sec. The true deflection is therefore proportional to $(0.054)^2 = 2.9 \times 10^{-3}$ while the deflection expected from the flask measurement would be proportional to 2.5×10^{-3}--an error of 15%. Thus an additional superfluid current that gives an immeasurably small deflection by itself can, when added to a larger current, produce a noticeable effect due to the quadratic dependence of the torque on the velocity.

Since by the nature of the experiment the filling time (t) provides the basic velocity determination, equation 10 can be expressed more significantly as

$$v_s = \frac{\rho\ V}{\rho_s\ A}\left(\frac{1}{t} + \frac{1}{t_o}\right). \qquad (12)$$

In this form, the quantity (t_o) represents physically the time required for one "flask-full" of liquid to traverse the experimental region on the basis of evaporative losses

only. As will be seen, the data areobtained in a form directly applicable to the experimental determination of t_o.

In a similar manner the factor $1/t$ in equation 9 must be replaced by $(1/t + 1/t_o)$ where t and t_o retain the same meaning as above. Taking the square root of both sides of the resulting equation gives

$$\sqrt{\theta} = \left(\frac{4}{3}\ \frac{a^3 \rho\, V^2}{\tau\, A^2}\ \frac{\rho}{\rho_s}\right)^{1/2} \left(\frac{1}{t} + \frac{1}{t_o}\right) \qquad (13)$$

which can be conveniently written as

$$\sqrt{\theta} = k\left(\frac{1}{t} + \frac{1}{t_o}\right) \qquad (14)$$

defining the temperature dependent constant k. The temperature dependence of k enters only through the $(\rho_s/\rho)^{-1/2}$ factor.

There will be a further discussion of equation 14 in section VII-A where it will be shown that this equation is not quite valid but is still used because it is correct to within the limits of the experiment and because its use simplifies the analysis.

The postulate that $1/t_o$ is a constant, independent of flow rate, will be made. This is done primarily for expediency; however, it can be justified. The evaporation rate should be constant if the temperature difference between the bath and the exhaust region is steady. According to the London equation this condition should prevail as long

as the bath level remains constant because there is then a constant pressure difference between the two regions. This result is independent of the flow rate.

As has been discussed previously, the bath level does not remain constant, but drops slowly due to evaporation of helium. Despite the fact that this lowering of the bath level produces a long term change in the fluid velocity, it is found experimentally that H_o remains constant within ten or twenty percent during the time required to take all the data at any one temperature. This implies that the evaporation rate and hence $1/t_o$ is constant to within the same amount. Since $1/t_o$ represents a velocity that is small compared to the flow velocity, a ten or twenty percent error in its determination is not important.

The idea that the lowering of the bath level produces a negligible variation in $1/t_o$ is not inconsistent with the fact that it causes a very obvious change in the flow rate over the same length of time. A comparison of equations 6 and 11 shows that evaporation is a less efficient method for producing superflow from heat than is the fountain effect by a factor of $Ts/(L + Ts)$. This factor has a maximum value of about 1/9 and gets very small at lower temperatures. Thus a quantity of heat that produces a small change in the evaporation current will produce ten or more times that change in the fountain effect current.

B) Statistical Analysis

The data taken in this experiment are the angular deflection θ and the filling time t. The problem of fitting a set of points $\sqrt{\theta}_i$ and $1/t_i$ to equation 14, assuming that k and $1/t_o$ are unknown constants, involves standard procedures in statistical analysis.

However, determining k and $1/t_o$ by fitting equation 14 has one defect. The statistical analysis method determines the constants that will give a minimum deviation. This over-weights the points with large values of $1/t$ which is where the errors of measurement are the greatest. It is the same statistical analysis problem to fit

$$\frac{1}{t\sqrt{\theta}} = -\frac{1}{t_o\sqrt{\theta}} + \frac{1}{k} \qquad (15)$$

except that for this curve the data points are $\frac{1}{t_i\sqrt{\theta}_i}$ and $\frac{1}{\sqrt{\theta}_i}$. To first order $\frac{1}{t_i\sqrt{\theta}_i}$ is a constant so that fitting equation 15 weights all the points approximately equally.

VI. EXPERIMENTAL RESULTS

A) Data

In appendix E all the data points Θ and t are listed together with the temperature at which each point was taken.

For each group of points the values of the average temperature $\overline{T}$ and of the constants determined by the statistical analysis $1/k$ and $1/t_o$ are given in table 1 as well as the value for $1/k^2$ which is proportional to ρ_s/ρ .

B) Torque Law

Figures 7, 8 and 9 are graphs of $\sqrt{\Theta}$ vs. $1/t$ at each nominal temperature. The straight lines drawn through these points are those given by the constants $1/k$ and $1/t_o$ as determined by the statistical analysis.

The graphs demonstrate the essential validity of equation 14; i.e., they show unequivocally the necessity of incorporating the constant t_o and they show that the torque (angular deflection) has a quadratic dependence on the velocity. Of course, the graphs themselves show that the square root of the torque depends linearly on the velocity.

Figure 10 is a graph of ρ_s/ρ vs. T as determined by this experiment. This was taken from the $1/k^2$ column of table 1. From equation 13 and 14 it is seen that

$$k^2 = 4/3 \frac{a^3\rho}{\tau} \frac{V^2}{A^2} = \frac{\rho}{\rho_s} .$$

TABLE 1

RESULTS OF STATISTICAL ANALYSIS

$T(^{\circ}K)$	$k(\text{sec-deg}^{1/2})$	$1/t_o(1/\text{sec})$	$1/k^2(\text{sec}^2\text{-deg})^{-1}$
1.17	17.9	0.0266	0.00314 ± 0.00028
136	18.6	0.0208	0.00290 ± 0.00027
1.44	18.9	0.0334	0.00281 ± 0.00028
1.51	20.3	0.0069	0.00243 ± 0.00035
1.59	21.2	0.0084	0.00222 ± 0.00022
1.66	21.1	0.0159	0.00225 ± 0.00021
1.77	18.2	0.0280	0.00300 ± 0.00022
1.77	19.8	0.0264	0.00255 ± 0.00022
1.86	22.2	0.0154	0.00203 ± 0.00011
1.89	22.9	0.0132	0.00191 ± 0.00011
1.92	22.3	0.0161	0.00201 ± 0.00008
1.97	25.9	0.0092	0.00149 ± 0.00016
2.02	25.9	0.0125	0.00149 ± 0.00012
2.08	33.7	0.0071	0.00088 ± 0.00011
2.10	34.5	0.0115	0.00084 ± 0.00006

Substituting the numerical values given previously gives

$$1/k^2 = 0.00247 \ \rho_s/\rho \ .$$

Using the correct value of $1/k^2$ gives a ρ_s/ρ curve that has a value of 1.08 at $T = 0^{\circ}K$. So, in the plotting of the graph of figure 10 the values for $k^2 \ \rho_s/\rho$ were normalized to give the correct result at zero degrees ($\rho_s/\rho = 1$). In section VII-B it will be shown that the influence of the walls of the wind tunnel could account for $1/k^2$ having too large a value.

VII. DISCUSSION

A) Difficulties in Zero Positioning

The method used for calibrating the optical system and checking the zero position on the scale was such as to make $\theta = 0$ when $1/t = 0$. Reference to the graphs of figures 7, 8 and 9 shows that extrapolating the data points will give θ a non zero value at $1/t = 0$-- usually between 0.1 and 0.2 degrees. For example the graph for $T = 1.66^{\circ}K$ shows that at $1/t = 0$, $\sqrt{\theta} = 0.34$ or $\theta = 0.1$. Thus, something is wrong with equation 14.

The trouble is that the angular deflections should have been measured from the point where the disk comes to rest when no heat is applied. Equation 14 is not really true when θ is measured as described previously. Unfortunately, it was experimentally impossible to use the true zero position because, when the heater was turned on after setting the zero position with no heat applied, the disk would receive a large impulse and certainty in the original position would be lost due to the hysterisis effect mentioned previously (section IV-E).

When θ is measured from the zero position used in the experiment ($\theta = 0$ when $1/t = 0$) equation 14 should be modified to read

$$\sqrt{\theta + \theta_o} = k(1/t + 1/t_o), \qquad (16)$$

introducing another parameter θ_o which is the deflection

caused by the superfluid flow represented by $1/t_o$. Since by definition $\theta_o = k/t_o$, squaring both sides of equation 16 gives

$$\theta = k^2 \left(\frac{1}{t^2} + \frac{2}{t\, t_o}\right).$$

This is in a form suitable for least squares analysis if the variables are considered to be $1/t^2\theta$ and $1/t\theta$.

Although technically correct the last mentioned equation was not used for analyzing the experiment. First because the corrections for θ of the order of 0.1 degree are within the experimental error. And also because there is another effect which has not been mentioned yet that destroys certainty in the relationship $\theta = 0$ when $1/t = 0$.

This effect is that for values of t of around 200 seconds or longer (at this point the liquid is dripping out of the exhaust spout) there is an oscillation of the liquid. It rises high enough to come out of the spout, immediately falls and then promptly rises again. The frequency of this motion is about three or four oscillations per second. The amplitude varies between three and five mm. The motion only took place on the inside of the three mm tubing. The disk rectified this AC fluid flow and was deflected as much as 0.3 degrees by it.

This same effect could take place any time the fluid level reached a portion of the tube where the diameter

increased with height. It was undoubtedly alternate over-heating and over-cooling of the liquid as it reached places where the evaporation rate was less or more.

It was also very difficult to find a setting that would keep the liquid level stationary in a straight portion of the exhaust tube. Due to the evaporation from the bath the liquid level slowly fell and a height that was stable often would not be so by the time the zero setting had been carefully made.

For all these reasons, any sophisticated method of data analysis that required an accurate knowledge of the zero position was not feasible and the simpler method previously described, which should be asymptotically correct, was used.

It is also possible that the disk rectified some of the AC component introduced by the instabilities in the fluid velocities.

B) Tunnel Wall Effects

It is clear that the torque equation (equation 1) which was derived for the case of an infinite medium is not completely valid as applied to this experiment. In this section an estimate of the correction necessitated by the effect of the walls of the wind tunnel will be made, but there will be no attempt to solve the complete problem. The correction factor that will specifically be

sought for is that necessary to explain why ρ_s as determined by this experiment has too large a value.

The most obvious effect of the walls is that of "squeezing in" the flow lines. This will result in a higher velocity in the vicinity of the disk than there would be in the case of an infinite medium. The torque, apart from geometric factors, is basically a measure of $\rho_s v_s^2$. In this experiment, the velocity used in the determination of ρ_s is essentially the velocity at infinity in the tube (v_1). What should have been used, to a first approximation, is a larger velocity (v_2).

If the subscripts 1 and 2 are used to denote the values of ρ_s that would be extracted from the experimental data using the velocity v_1 and the (truer) velocity v_2 respectively we can say

$$\rho_{s_1} v_{s_1}^2 = \rho_{s_2} v_{s_2}^2 .$$

Thus, in order to obtain the correct value for ρ_s (ρ_{s_2}), the values of ρ_s (ρ_{s_1}) already obtained from the table of $1/k^2$ (table 1) must be multiplied by a factor $v_{s_1}^2/v_{s_2}^2$.

The value of this factor can be estimated from conservation of current simply by assuming that the ratio v_{s_1}/v_{s_2} will be inversely proportional to the ratio of the area of the wind tunnel with no disk present to the area available for the fluid to go through (at the disk) with

the disk present. If a is the radius of the disk its projected area when $\alpha = 45^{\circ}$ is $\frac{\pi a^2}{\sqrt{2}}$. Now, if b is the radius of the tunnel, the total area of the tunnel is πb^2 and the available area at the disk is $\pi b^2 - \pi a^2 (2)^{-1/2}$. Thus, to this approximation,

$$\frac{v_{s_1}}{v_{s_2}} = \frac{b^2 - a^2/\sqrt{2}}{a^2} .$$

Using the values b = 0.5 cm and a = 0.15 cm gives the result

$$\frac{v_{s_1}}{v_{s_2}} = .935$$

or

$$\rho_{s_2} = 0.87 \ \rho_{s_1} .$$

Multiplying by this factor does bring the experimental values of ρ_s down to roughly the correct value.

VIII. CONCLUSION

The torque produced by liquid helium II flowing through a superfluid wind tunnel has been determined over a range of velocities varying by a factor of about ten. The velocity dependence of the torque at any one temperature is shown to be consistent with that predicted by classical hydrodynamics, providing a few assumptions regarding the wind tunnel's behavior are made. The variation of the torque with temperature is in accord with the two-fluid model of liquid helium. Thus the conclusions must be drawn that the operation of the wind tunnel is essentially as would be expected from the two fluid model and that the hydrodynamical behavior of superfluid is the same as that of an ideal classical fluid in this case.

The variation of the torque with temperature while a constant exhaust flow rate is maintained is a particularly dramatic effect even though it is expected because such a behavior so clearly indicates the unusual nature of liquid helium.

APPENDIX A

The Theory of Landau

This section is not meant to be a review of liquid helium theory but is merely intended to give an indication of the derivation of two fluid model from the theory of Landau; consequently, the Bose Einstein condensation and other topics in liquid helium theory will not be treated.

In a paper in 1941 (2) Landau laid the foundations for the modern theory of liquid helium II. Some parts of Landau's original work have later proven wrong and much more of it was completely empirical. Later workers, particularly Feynman (3) and Feynman and Cohen (9), have since established several speculations of Landau's.

The essence of today's theory is that at absolute zero the assembly of helium atoms is in a ground state and that, as the temperature is increased, excitations, which are states of the whole system, appear. An important point is that states of the whole system are considered rather than the motion of individual atoms. The excitations have an energy-momentum spectrum as shown in figure 11.

All the thermodynamical properties of liquid helium can be derived from this energy spectrum by the usual methods of thermodynamics. In this derivation only two

parts of the curve contribute significantly due to the low temperatures involved. These are drawn with a solid line in the figure and are labeled phonon and roton.

The energy-momentum spectrum can be approximated in the phonon region as

$$E = cp \tag{17}$$

where c is the speed of sound, and in the roton region as

$$E = \Delta + \frac{(p-p_o)^2}{2\mu} \tag{18}$$

where Δ, μ, and p_o are parameters which are chosen by fitting theoretical thermodynamical functions to their measured values. The values obtained are $\Delta/k = 9.6^oK$, $\mu/m_{He} = 0.77$ and $p_o/\hbar = 1.95 \times 10^8/cm$. Feynman and Cohen's derivation gives a value of $\Delta/k = 11.5^oK$.

Derivation of the Two Fluid Model

By a Galilean transformation of the wave function of an excitation in the fluid it can be shown that, if the fluid is moving at a velocity $\vec{v}$, the energy (E_o) in a stationary co-ordinate system of an excitation, which has an energy E in the system in which the fluid is at rest, is

$$E_o = E + \vec{p} \cdot \vec{v} . \tag{19}$$

The derivation of this is discussed by Dingle (10).

It can be seen that the excitations with their momentum directed oppositely to the velocity of the fluid will have less energy and hence greater statistical weight than

excitations with their momentum directed along the velocity. Thus, the gas of excitations will appear to move with less velocity than the background fluid.

More specifically, if the background is moving with a velocity v_1 in a tube that is moving with velocity v_2, and if the excitations are in equilibrium with the walls of the tube, statistical mechanics gives the equilibrium distribution of the excitations as

$$n(E) = \exp \frac{E_o - \vec{p} \cdot \vec{v_2}}{k\,T} - 1 \quad ^{-1},$$

assuming Bose statistics.

Using equation 19 to eliminate E_o, the net momentum associated with the excitations can be computed using

$$\vec{p} = \frac{1}{(2\pi\hbar)^3} \int \vec{p}\; n(\vec{p}\;) d^3\vec{p}$$

$$= \frac{1}{(2\pi\hbar)^3} \int \vec{p}\; \exp \frac{1}{kT}(E(p) + \vec{p} \cdot \vec{v_1} - \vec{p} \cdot \vec{v_2}) - 1 \quad ^{-1} d^3\vec{p}\,.$$

If the assumption is made that v_1 and v_2 are small, this integral can be evaluated as

$$\vec{p} = - \text{const}(\vec{v_1} - \vec{v_2}) \,. \qquad (20)$$

The constant in equation 20 is a positive quantity with the dimensions of density; and, in this approximation, is a function only of temperature (i.e., not of velocity).

The total momentum per unit volume $\vec{j}$ possessed by the moving liquid will then be

$$\vec{j} = \rho \vec{v_1} - \text{const.}(\vec{v_1} - \vec{v_2}).$$

That is, the usual momentum plus the momentum associated with the excitations.

If the constant is now called ρ_n, v_1 and v_2 called v_s and v_n, respectively, and a parameter ρ_s defined by

$$\rho = \rho_n + \rho_s$$

the simple expression

$$\vec{j} = \rho_s \vec{v_s} + \rho_n \vec{v_n}$$

results.

This is a statement of the two fluid model discussed in the introduction.

This derivation is essentially that given by Wilks (11).

APPENDIX B

Validity of Calibration Procedure

In this Appendix it will be shown that accurate results are obtained from the calibration procedure described in section IV-E despite the presence of the unknown perturbing torque caused by the magnet. More specifically, it will be shown that if the disk assembly is suspended from a fiber of torsion constant τ in the presence of an arbitrary perturbing torque, the disk will be rotated by the same amount (θ') when it is acted upon by a torque of magnitude $\tau\theta$ as when the fibers support is turned through an angle θ.

A series of drawings (figure 12) has been made to assist in this proof. In drawing (a) the plane of the disk is lined up at an angle α to some arbitrary line with no external torque applied. When the magnet is added the torque it produces will change the alignment of the disk so that it now makes an angle β with the same line. This is illustrated in drawing (b). If the torque caused by the magnet is some arbitrary function of position of the disk $L_M(\phi)$, the angle β is determined by the relationship

$$L_M(\beta) = \tau(\beta - \alpha) .$$

If the pointer is rotated counter-clockwise through an

angle Θ, the disk will rotate through an angle Θ' such that

$$L_M(\beta + \Theta') = \tau(\beta - \alpha - \Theta + \Theta') . \qquad (21)$$

Drawing (c) makes this clear. The disk would be at $\alpha + \Theta$ without the perturbing torque, instead it is at $\beta + \Theta'$ so that the restoring force of the fiber is opposing a rotation of $(\beta + \Theta') - (\alpha + \Theta)$ caused by the magnetic torque.

With the disk again in position (b) a torque L acting on the disk (i.e., one caused by the fluid flow) will rotate the disk through an angle Θ'' such that

$$L_M(\beta + \Theta'') + L = \tau(\beta + \Theta'' - \alpha) \qquad (22)$$

This is shown in drawing (d). In this case the net displacement of the disk from the equilibrium position is $\beta + \Theta'' - \alpha$ and the torques causing this displacement are L and $L_M(\beta + \Theta'')$.

It is obvious by inspection that if $L = \tau\Theta$, $\Theta' = \Theta''$ is a solution of equations 21 and 22. Depending on the shape of L_M other solutions are possible, but in practice these correspond to complete rotations of the disk and so would be easily discovered by the experimenter.

ATTEMPTS TO ELIMINATE INSTABILITY

APPENDIX C

This Appendix will be a discussion of various attempts that were made to eliminate the instability of the disk's motion.

It was found that there was some vibration communicated to the dewar through the vacuum pump line and a device was built to decouple the line from the dewar. This did stabilize the disk somewhat, but more elaborate decoupling both from the pump line and from other possible external sources of vibration would not decrease the vibrations further. It was therefore concluded that the remaining instabilities were not caused by vibrations of the dewar. Basic to such a conclusion was the fact that the disk remained perfectly still when there was no fluid flow.

There was no difference in the disk's behavior with the forward superleak present or absent. Likewise, using a device to smooth the flow in the forward end of the wind tunnel produced no effect.

On one occasion, the whole wind tunnel was painted black (with the exception of a small section left transparent for optical purposes) to eliminate any effects due to stray radiation. This produced no effect as could probably have been deduced from the fact that a flashlight shined on the superleak and turned on and off did not cause a noticeable difference in the disk's behavior. Similarly,

varying the intensity of the light source used for the deflection measurements made no difference.

Flow irregularities could also have resulted from an erratic heat supply. This could happen in three ways. First, the voltage or current supplied to the resistor could change; second, the value of the resistance itself could change; and third, the heat could escape unevenly from the resistor.

The first and second possibilities are easily investigated by measuring the voltage across and the current through the resistor. Performing such a measurement revealed nothing. These measurements were not made critically; however, the velocity variations were really large scale and would have required at least a 5% variation in the heat input for their production.

Determining the constancy of heat escape from the resistor is difficult; however, a good argument can be made that heat escaping erratically from the resistor would have produced flow irregularities different than those actually observed. The heat that really drives the wind tunnel is the total heat input (H) less the heat lost by evaporation (H_o). Now, when H is just slightly greater than H_o, a small variation in H would produce a large relative change in the total heat available to drive the tunnel, whereas, when H is large compared to H_o a similar variation in H will not produce as great a relative change in the net heat input. On

this model, greater irregularities would be observed for small deflections, which is exactly opposite from the behavior actually noted.

Furthermore, observations were made for two different values of H_o. As stated in section IV-B, before modifying the exhaust spout H_o was about 0.2 watts and afterwards it was about 0.01 watts. The maximum heat actually used to drive the tunnel was 0.015 watts. Thus, heat escaping erratically from the resistor before the exhaust spout modification was made would have produced very large variations in the net heat input. In practice, the instabilities in the disk's motion were virtually the same before and after H_o was minimized thus eliminating the objection that the erraticness of heat escape could vary with heat input in just such a way as to produce the velocity variations noted. The above arguments can also be applied in the cases of noisy resistors or voltage or current variations.

In addition to this, Pellam and Craig (5) experimented with various types of resistors in an effort to stabilize the flow, but obtained no positive results. Because of all the above, it was concluded that the heat source used in this experiment was adequate and that the flow irregularities were not due to a variable heat input.

There are two additional sources of heat input variations. The first of these is variable heat conduction from the bath to the exhaust region through the path provided by

the exhausting fluid. This was investigated by shaping the exhaust spout like a fountain so that the fluid would spray out and any possible conduction path would be broken up. This also produced no effect.

The second possibility, which was not investigated, was changes in the evaporation rate caused by the fact that the fluid does not come out of the exhaust spout evenly and so does not present a constant area for evaporation. Again, the changes in flow rate are on a much larger scale than should be produced by this mechanism. A method of constructing the exhaust spout that should eliminate this problem and would have some additional virtues is given in Appendix D.

One method of stabilizing the flow based on the idea that the velocity changes would be accompanied by changes in the temperature of the exhaust region was tried. This idea made use of the fact that the resistance of ordinary Allen and Bradley resistors is very temperature dependent at low temperatures. An AC resistance bridge was constructed with one limb of the bridge in the bath and the other in the exhaust region of the wind tunnel. The bridge was balanced so that a decrease in temperature in the exhaust region would cause a greater signal output; this signal could then be amplified and fed back through another resistor to counteract the original change in temperature.

In practice, it was found that the erraticness of flow was not accompanied by any detectable changes of temperature in the exhaust region. This was not due to lack of sensitivity of the bridge. The bridge was sensitive enough to easily detect the heating effect of a flashlight shined into the dewar, while doing the same thing would not affect the disk noticeably. The attempt to use inverse feedback to stabilize the flow was then abandoned.

APPENDIX D

Suggestions for Future Research

Both of the experiments that have been performed to date using superfluid wind tunnels have suffered from a lack of accuracy caused by the wind tunnel's erratic behavior. At present it is not known whether the variable flow rate will accompany superfluid flow through superleaks in general or whether it is only a feature of flow through carborandum powder or jewelers rouge superleaks. Clearly, one avenue of future research is the investigation of high volume flow of superfluid through superleaks.

In the past, superleaks have frequently been constructed by separating optically flat quartz plates by the appropriate distance (on the order of 10^{-5} cm). A superleak for this experiment could be made, therefore, by stacking many such quartz plates on top of each other. The critical flow velocities through these slit superleaks are of the order of 10 cm/sec. Thus, if the stack had a total area of 1 cm^2, it would have to be at least 1% hole before a volume flow rate of 0.1 cc/sec (as used in this experiment) could be achieved. This would require using about 1000 10^{-3} cm thick quartz plates and would clearly be almost impossible to do.

However, vycor glass has a uniform channel width in the neighborhood of 10^{-5} cm and is at least an order of magnitude more transparent than is required. Therefore, a wind tunnel should be constructed using a vycor glass superleak. If erraticness of flow is still observed it can probably be concluded that such erraticness will occur in general in a superfluid wind tunnel and the problem of smoothing the flow somehow must then be faced.

As was mentioned in Appendix C, it is possible that some of the flow irregularities are caused by unevenness in the evaporative heat loss rate because of the turbulent manner in which the fluid leaves the exhaust region. This could be eliminated by a modification of the exhaust spout.

This modification would be effected by making two basic changes in the design of the exhaust spout shown in E, figure 3. First, the tube through which the fluid escapes would be constricted to a diameter such that a pressure head of, say, five cm of helium would be required to produce a volume flow of 0.3 cc/sec (the largest used in this experiment) through it. Second, the tube extending upwards from the exhaust spout would be lengthened to five or ten cm.

The difference in the operation of the wind tunnel when an exhaust spout as described above is employed is obvious. The flow rate through the spout is now determined by height of helium in the column above it. The helium level will be the height where the temperature difference between

the exhaust region and the bath is such that the heat lost by evaporation plus that carried away by the exhausting fluid is equal to the heat supplied. The evaporation rate should now be constant for any given helium level because the evaporation will take place from surfaces of constant area--the cross section of the tube extending above the exhaust spout plus that of the spout.

If this construction does not help smooth the velocity variations it should at least eliminate the zero positioning difficulties described in section VII-A. It will also make it possible to follow variations in the flow rate by a means other than watching the motion of the disk. A change in the velocity should cause the liquid level above the spout to change because the amount of fluid that can flow through the spout is limited instantaneously by the pressure head above it.

This opens up another interesting possibility. If the change in pressure head is accompanied by a change in the temperature in the exhaust region, the inverse feedback smoothing device described in Appendix B should now work. The feasibility of this device depends, of course, on whether the response times of the sensing elements etc. involved are sufficiently rapid as well as on whether the wind tunnel would operate in the manner imagined.

It is felt that improving, for instance, the accuracy of the optical system by a factor ten would not be worth while until the wind tunnel's behavior can be stabilized.

APPENDIX E

EXPERIMENTAL DATA

Date	T	θ	t	Date	T	θ	t
April 22	1.166	1.6	24.6	April 15	1.503	0.8	29.2
"	1.166	2.5	16.1	"	1.507	2.0	16.9
"	1.166	3.7	13.6	"	1.506	3.6	12.6
"	1.166	5.8	9.0	"	1.508	5.7	9.7
"	1.166	1.6	21.3	"	1.510	7.6	7.6
"	1.166	2.3	16.2	"	1.511	1.0	20.8
"	1.166	3.6	12.3	"	1.518	3.0	11.7
"	1.166	4.3	10.8	"	1.521	6.4	7.9
"	1.166	6.1	8.5	"	1.512	4.9	9.8
"	1.166	3.3	14.7	"	1.503	1.9	17.3
April 22	1.366	1.4	23.0	April 15	1.587	0.9	29.0
"	1.366	3.0	14.8	"	1.600	3.0	12.3
"	1.366	5.0	10.7	"	1.587	5.0	10.7
"	1.366	7.5	7.8	"	1.584	3.1	14.2
"	1.366	3.4	13.3	"	1.574	0.7	30.5
April 20	1.361	2.3	17.4	"	1.582	1.7	19.7
"	1.355	3.2	13.0	"	1.587	3.1	13.3
"	1.353	5.0	9.5	"	1.578	5.6	10.0
"	1.353	3.5	11.5	"	1.600	2.3	16.7
July 31	1.444	0.9	53.1	April 6	1.662	1.1	32.6
"	1.449	2.0	25.0	"	1.662	3.5	13.4
"	1.437	3.2	16.5	"	1.670	5.6	10.5
"	1.437	2.9	21.5	"	1.662	3.0	15.8
"	1.437	4.9	12.5	"	1.668	1.1	26.6
"	1.437	3.6	15.7	"	1.662	5.9	9.4
"	1.437	4.0	13.2	"	1.662	3.8	13.5
"	1.444	5.5	10.6	"	1.662	2.8	15.7
"	1.444	6.0	9.4	"	1.668	2.0	20.2
"	1.437	2.7	17.6				

Date	T	θ	t	Date	T	θ	t
May 3	1.770	0.9	39.2	March 21	1.892	1.5	25.4
"	1.772	2.0	19.6	"	1.892	4.2	13.7
"	1.772	3.0	16.4	"	1.888	2.3	19.5
"	1.768	4.3	12.2	"	1.878	5.5	10.6
"	1.768	5.1	10.5				
"	1.770	6.0	9.5	March 24	1.917	1.4	28.1
"	1.772	7.1	8.3	"	1.921	3.4	15.3
"	1.763	1.8	23.2	"	1.924	7.1	9.2
"	1.770	2.8	15.5	"	1.921	5.0	11.8
"	1.768	6.0	8.7	"	1.919	3.2	15.2
				"	1.921	1.7	23.6
June 29	1.768	0.5	113.0	"	1.926	2.5	18.5
"	1.770	1.0	44.1	"	1.929	4.3	12.7
"	1.770	1.5	28.7	"	1.908	3.2	16.0
"	1.761	2.0	24.7				
"	1.772	2.4	18.7	March 21	1.974	2.8	17.9
"	1.770	3.1	16.6	"	1.962	4.1	15.2
"	1.768	4.2	12.5	"	1.975	6.5	10.7
"	1.768	5.2	11.5	"	1.967	1.7	26.5
"	1.772	7.0	8.8	"	1.978	3.0	19.6
"	1.764	3.0	17.5	"	1.975	1.3	28.6
				"	1.971	2.0	20.9
May 8	1.859	2.3	19.1	"	1.971	3.3	15.9
"	1.865	1.2	31.2	"	1.974	5.3	12.7
"	1.865	3.5	14.9				
"	1.864	4.7	11.9				
"	1.864	5.9	10.4				
"	1.864	7.4	8.6				
"	1.873	0.5	55.5				

Date	T	Θ	t
April 20	2.015	0.9	47.2
"	2.016	1.8	25.0
"	2.015	2.9	19.6
"	2.017	3.9	15.9
"	2.017	4.9	13.6
"	2.016	6.1	12.0
"	2.016	0.8	41.2
"	2.016	3.9	16.0
"	2.016	6.4	11.4
March 21	2.076	5.1	17.2
March 24	2.076	1.1	38.1
"	2.078	2.8	24.4
"	2.076	5.7	14.4
"	2.070	4.0	18.4
"	2.082	3.4	20.7
"	2.080	2.0	23.6
"	2.074	7.0	13.1
"	2.078	4.4	19.6
April 20	2.105	0.9	59.0
"	2.105	1.9	35.1
"	2.105	3.1	26.1
"	2.105	4.0	21.5
"	2.098	4.9	18.0
"	2.105	6.2	15.8
"	2.106	7.7	14.7
"	2.093	1.0	64.5
"	2.106	3.5	23.5
"	2.109	6.0	17.1

APPENDIX F

F I G U R E S

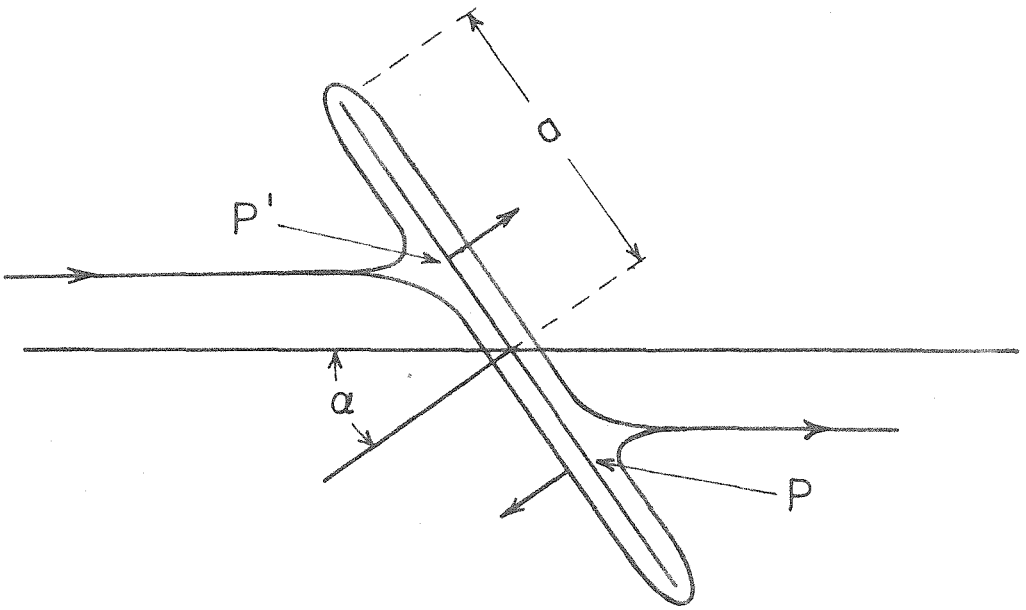

FLOW PATTERN AROUND A DISK

FIGURE 1

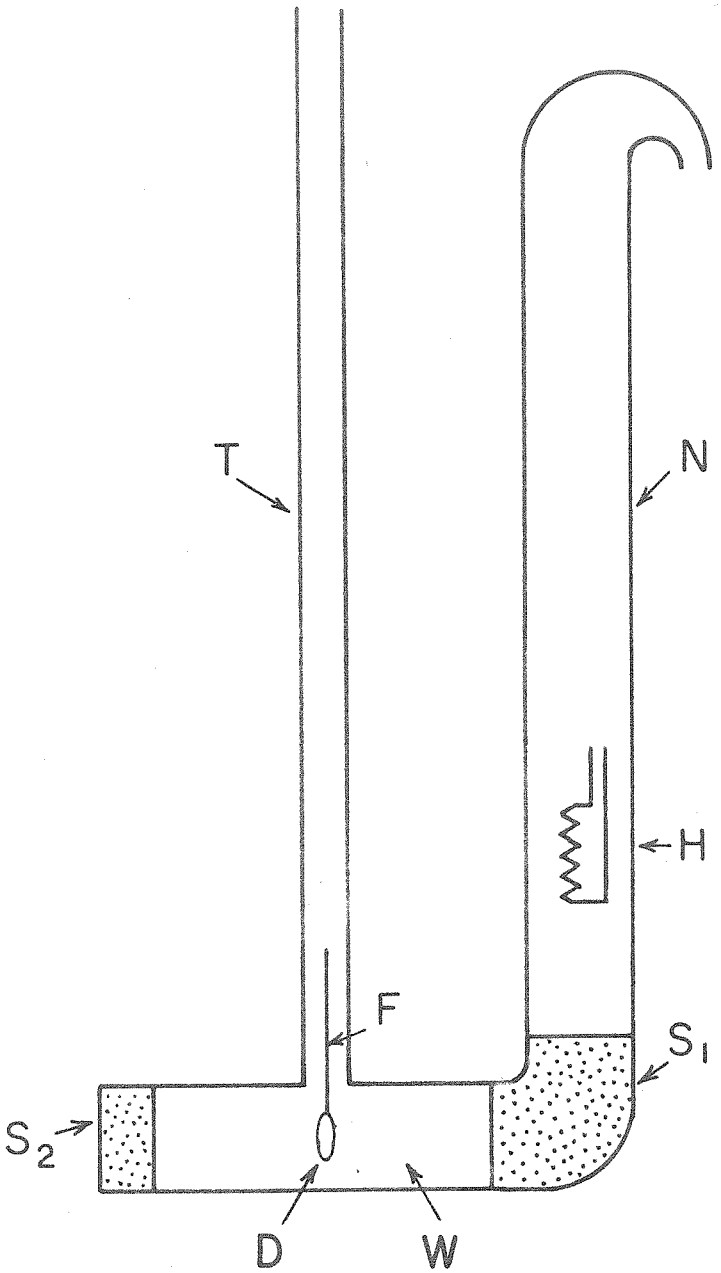

IDEALIZED SUPERFLUID WIND TUNNEL

FIGURE 2

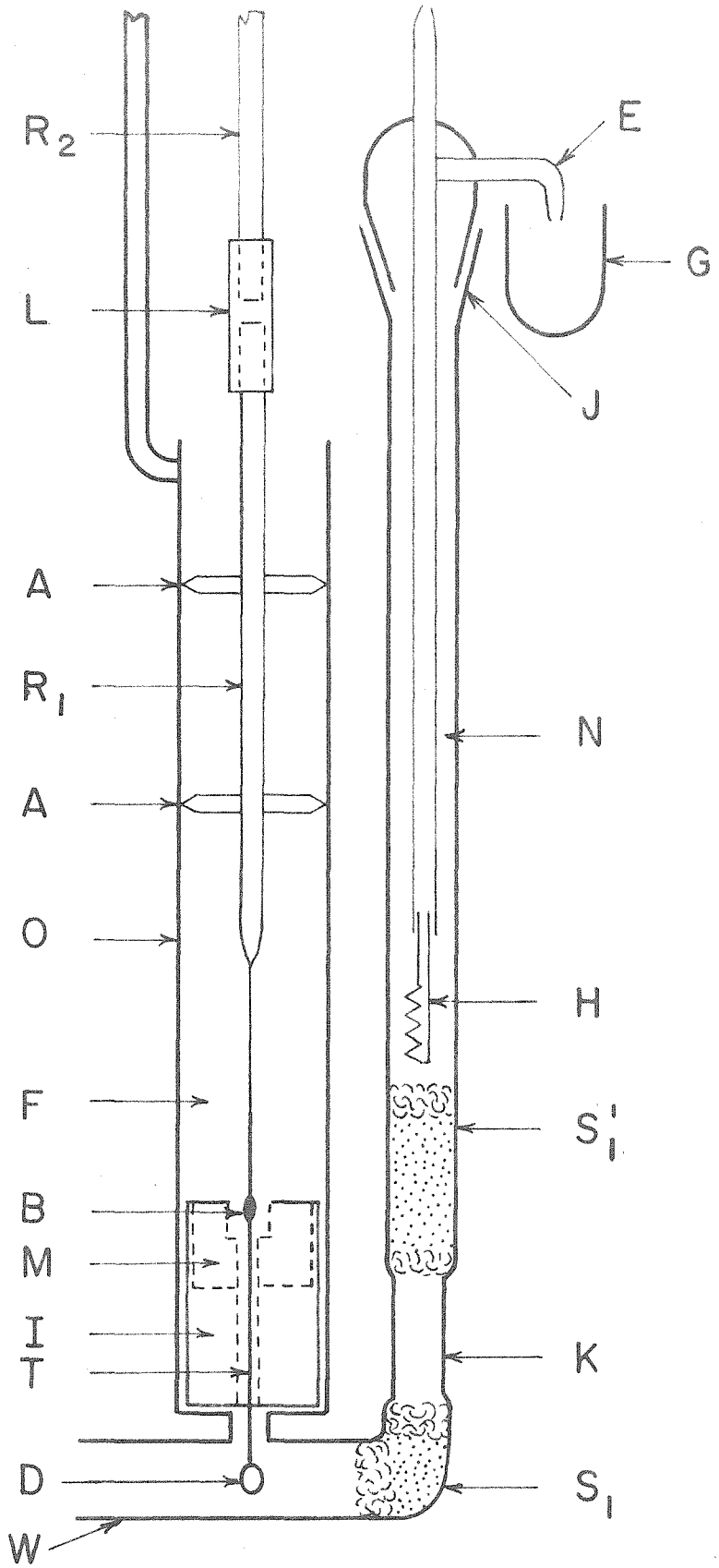

SUPERFLUID WIND TUNNEL

FIGURE 3

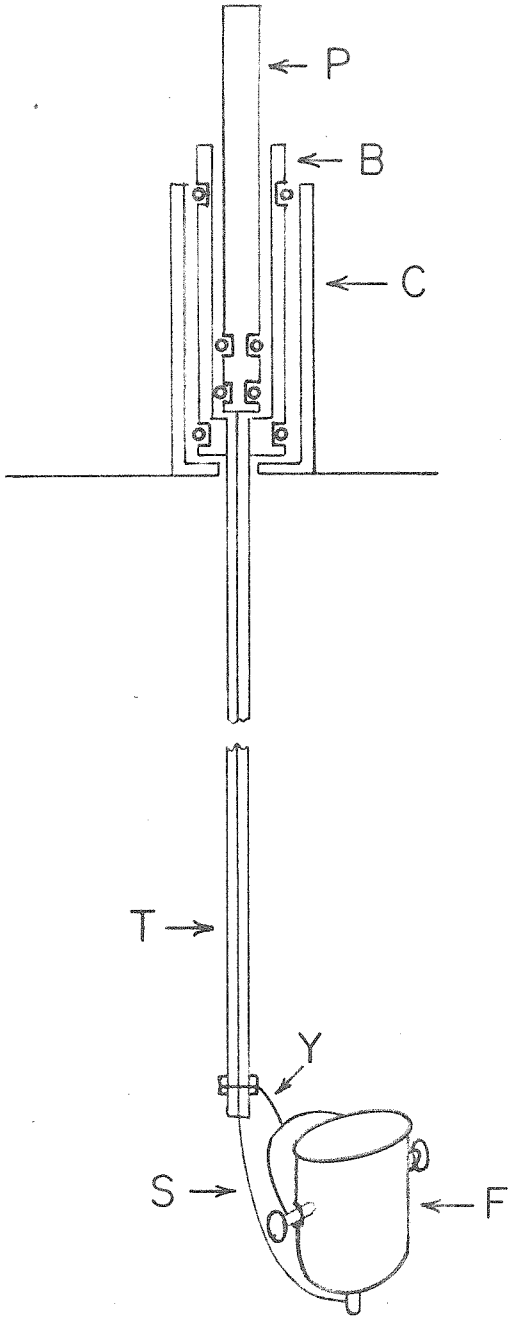

FLASK ASSEMBLY

FIGURE 4

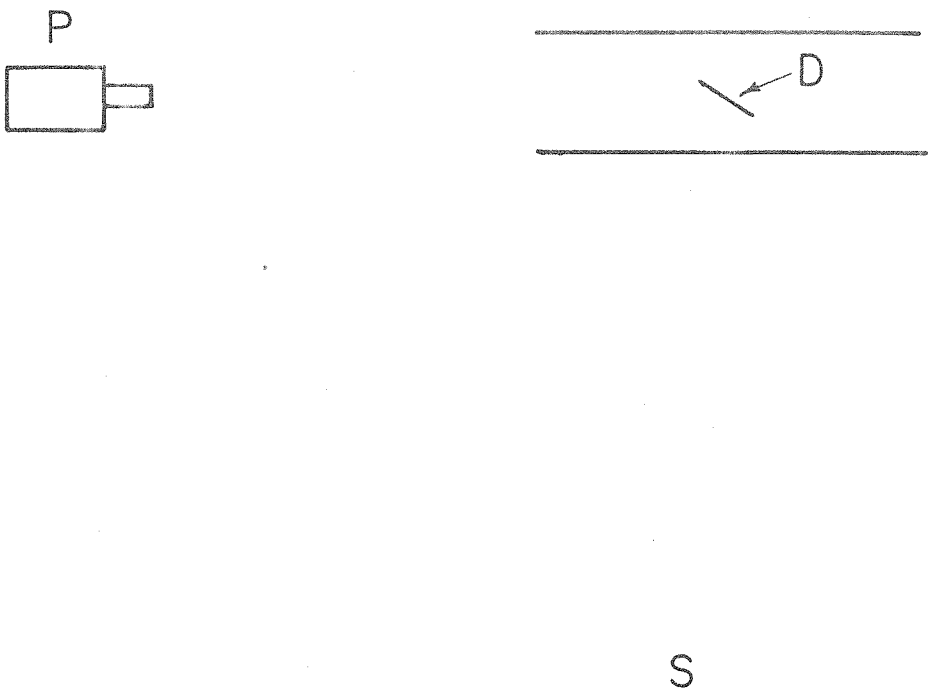

OPTICAL SYSTEM

FIGURE 5

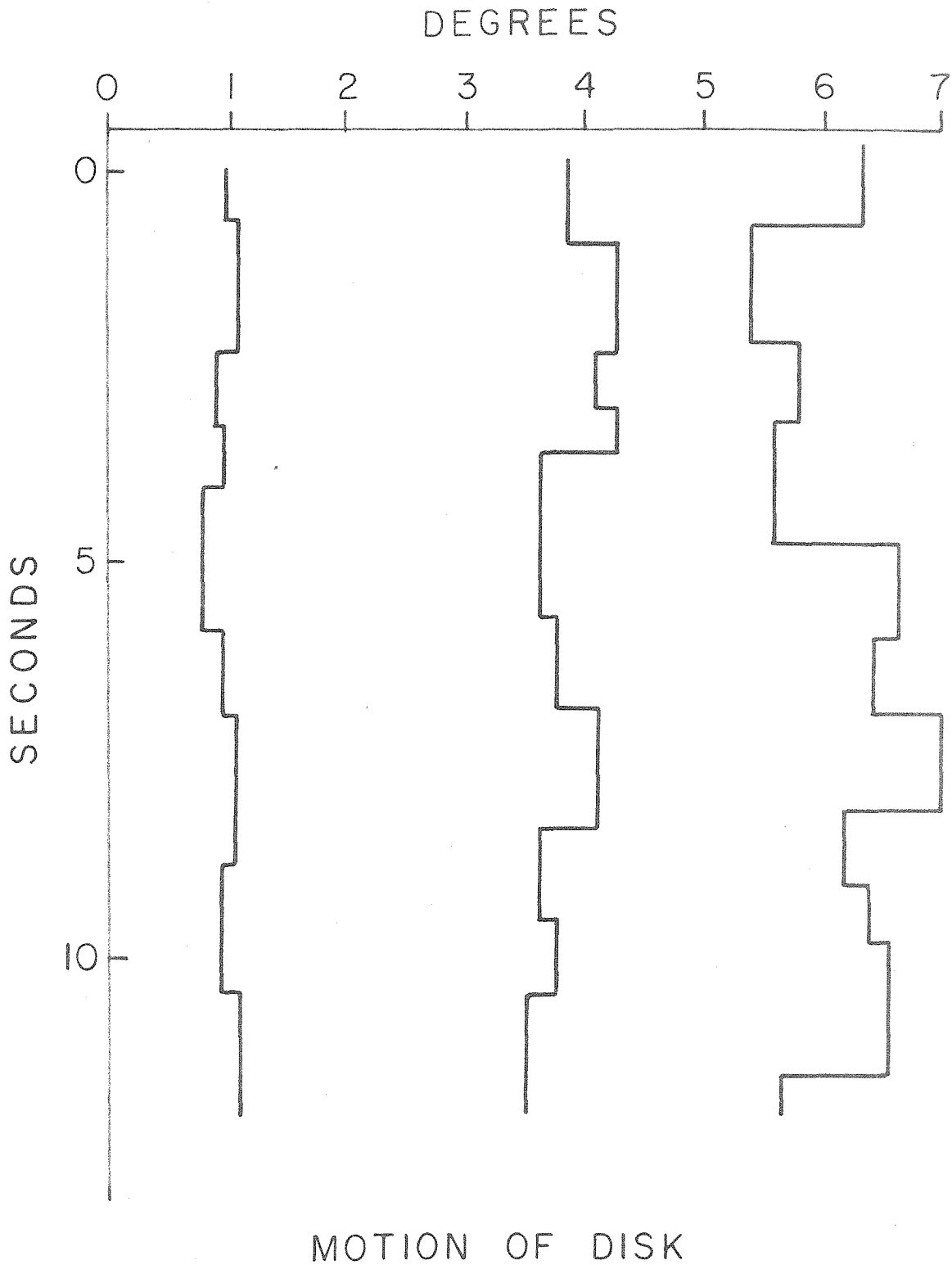

FIGURE 6

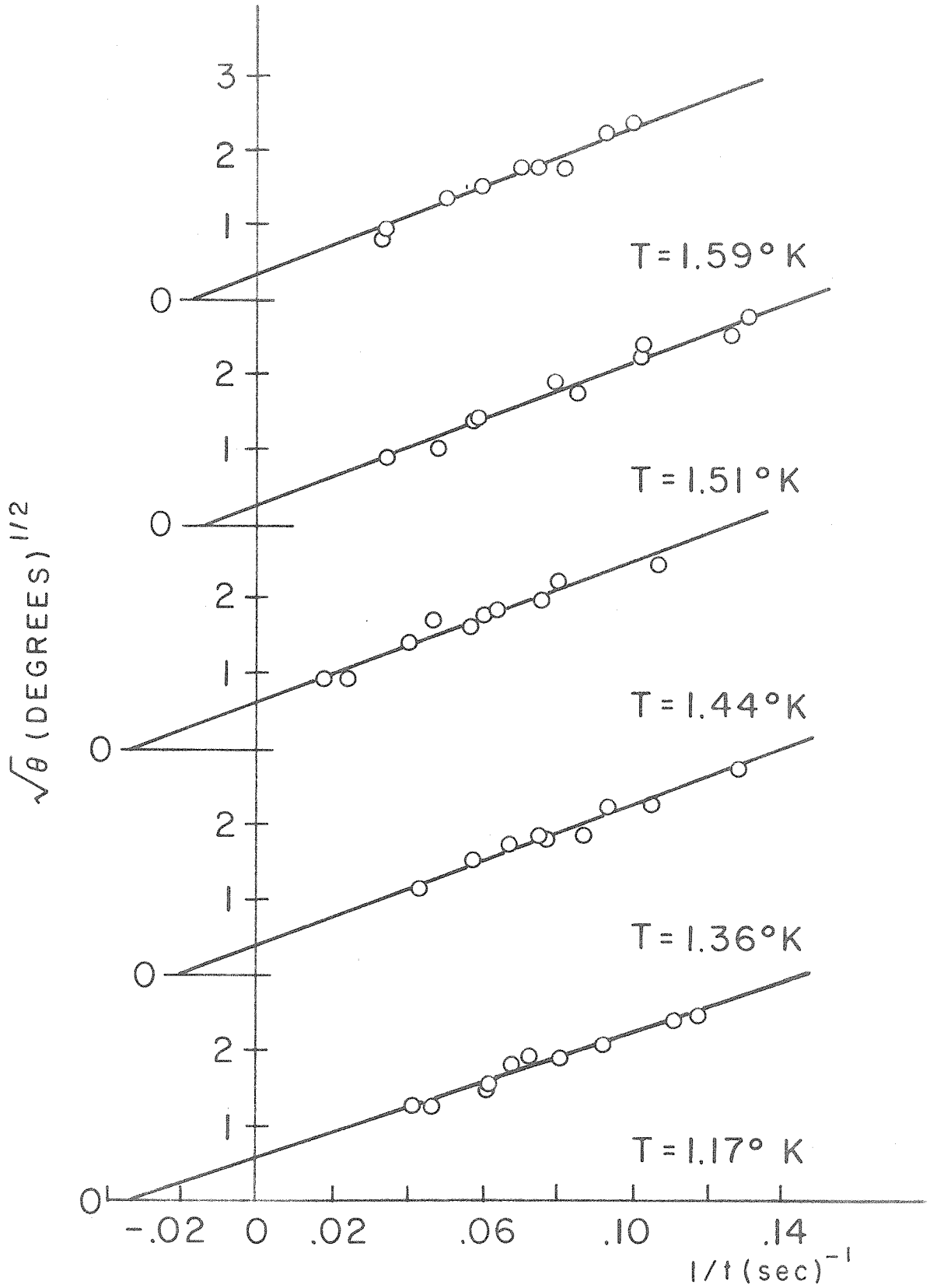

DEPENDENCE OF DEFLECTION (θ) ON FILLING TIME (t)

FIGURE 7

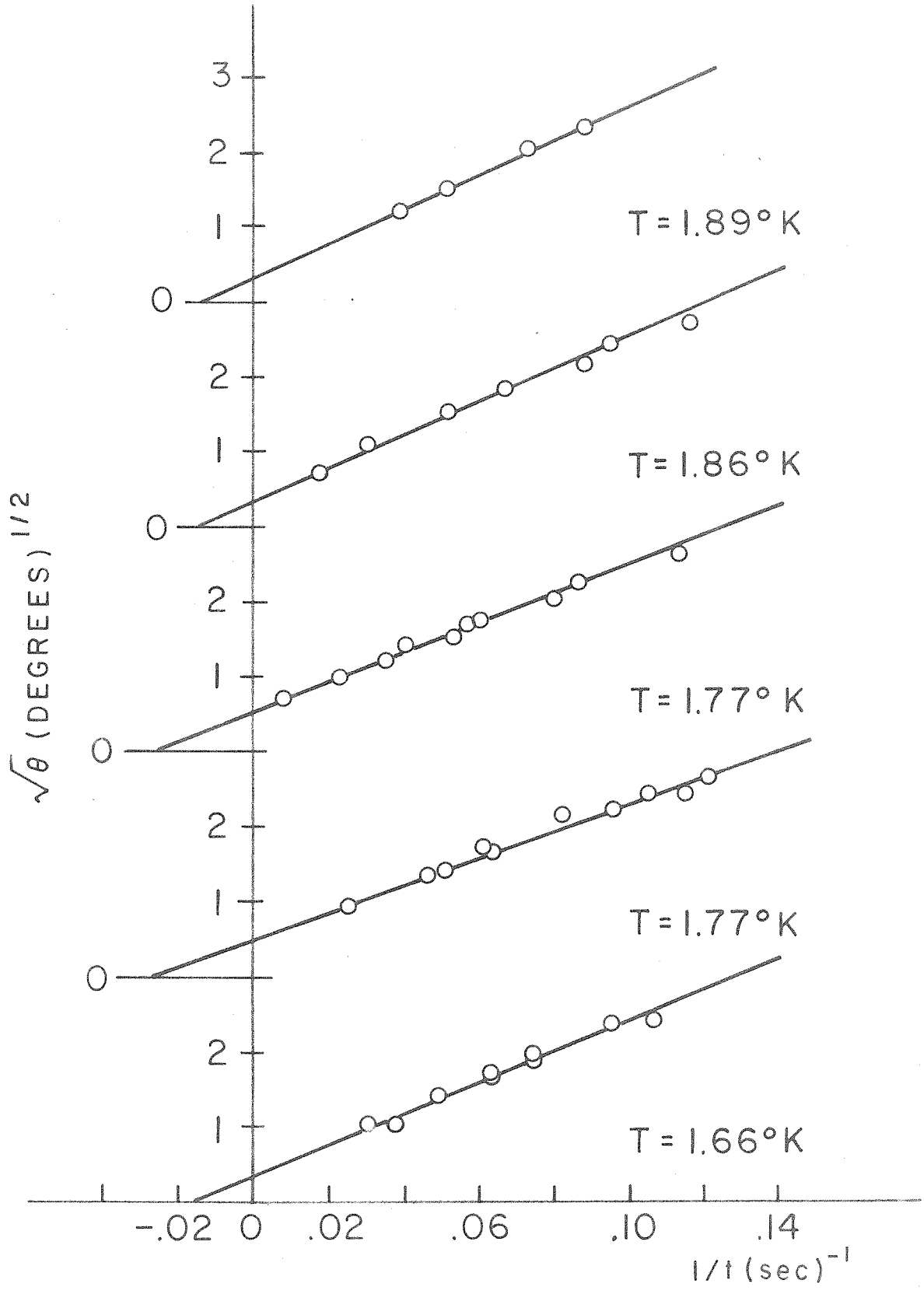

DEPENDENCE OF DEFLECTION (θ) ON FILLING TIME (t)

FIGURE 8

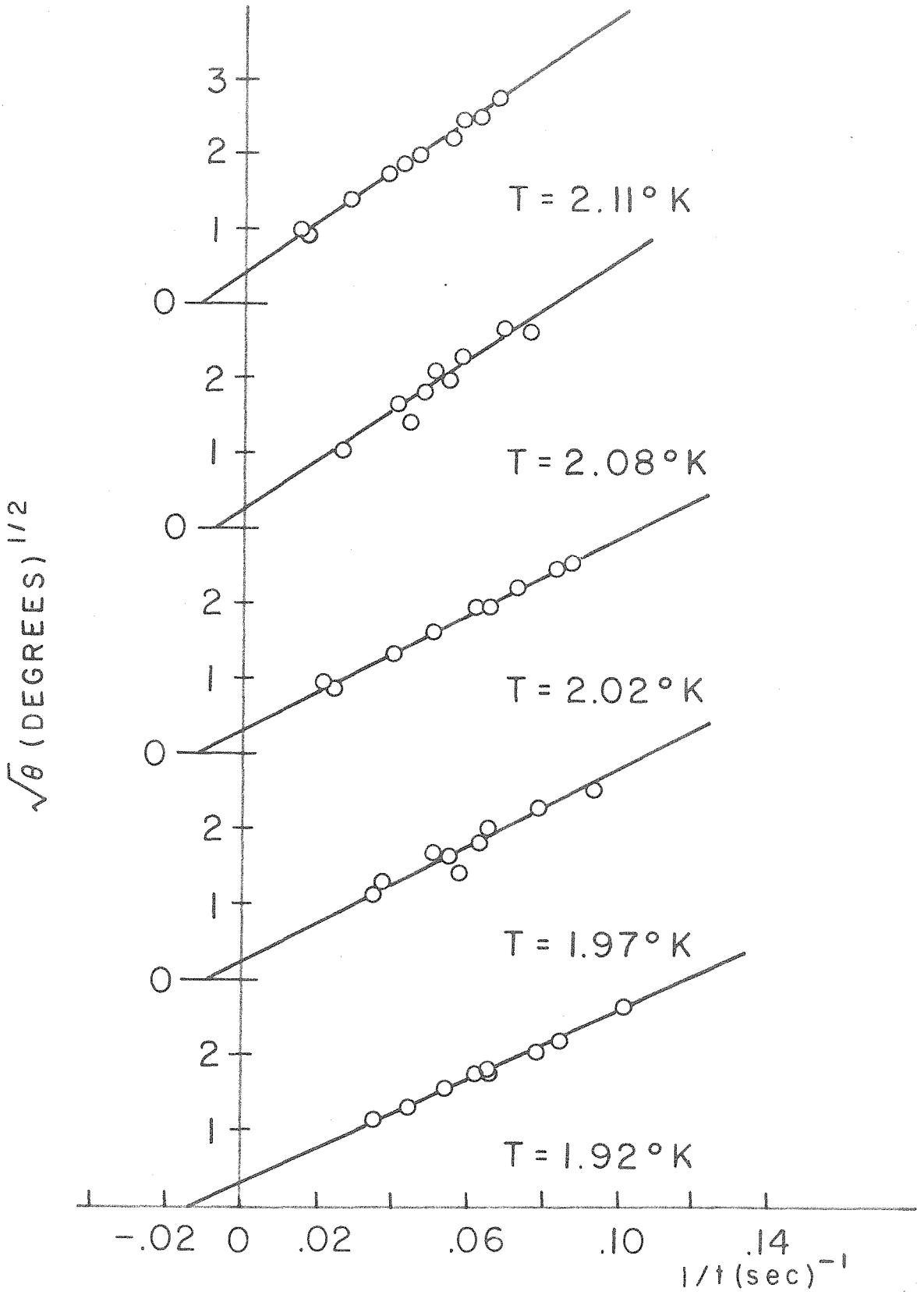

DEPENDENCE OF DEFLECTION (θ) ON FILLING TIME (t)

FIGURE 9

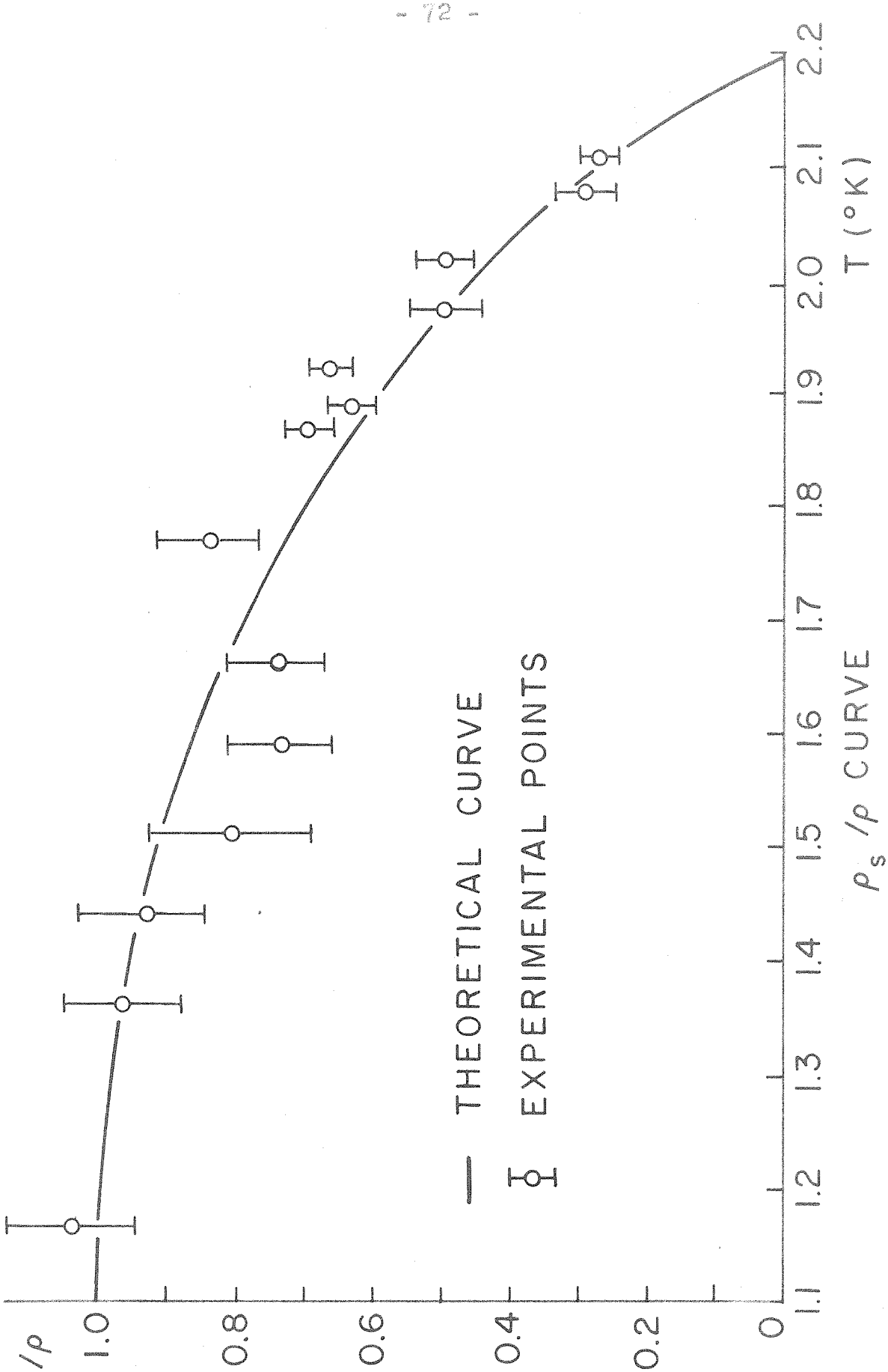
ρ_s/ρ
1.0
0.8
0.6
0.4
0.2
0
1.1
1.2
1.3
1.4
1.5
1.6
1.7
1.8
1.9
2.0
2.1
2.2
T (°K)
THEORETICAL CURVE
EXPERIMENTAL POINTS
ρ_s/ρ CURVE

FIGURE 10

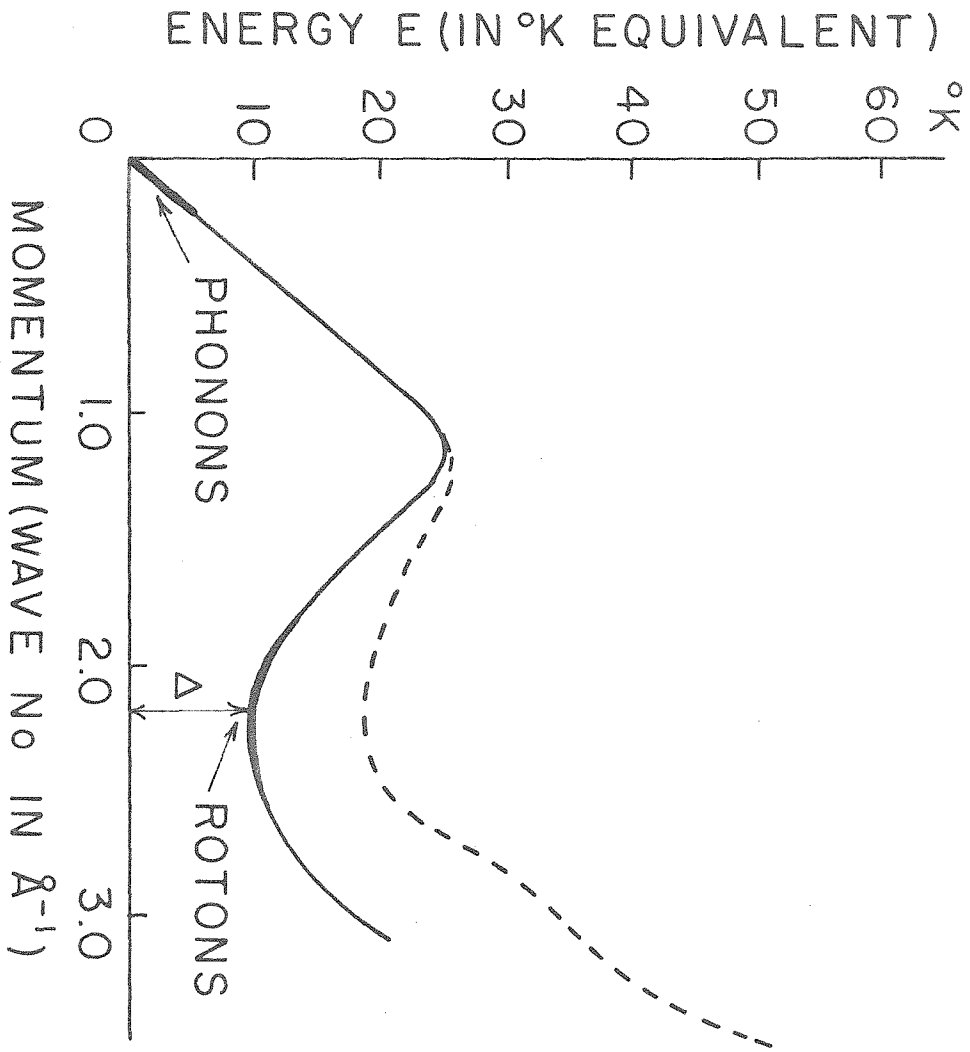

EXCITATIONS IN LIQUID HELIUM

FIGURE 11

(a)

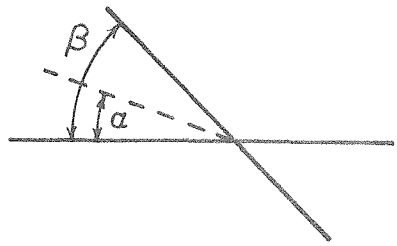

(b)

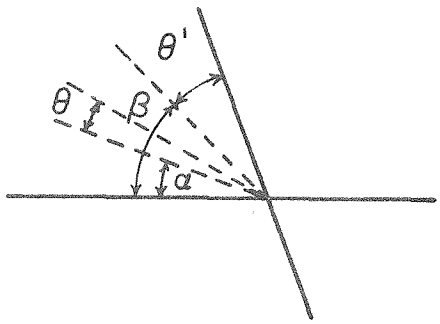

(c)

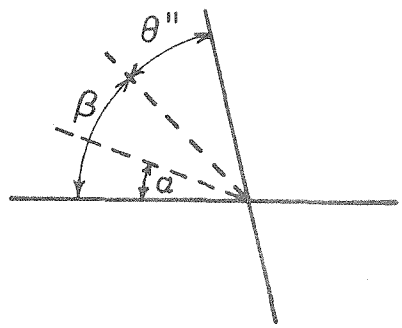

(d)

INFLUENCE OF MAGNET ON DISK

FIGURE 12

REFERENCES

1. Tisza, C. R., Phys. Rev., 72, 838 (1947).

2. Landau, L., J. Phys. USSR, 5, 71, (1941).

3. Feynman, R. P., in Progress in Low Temperature Physics, C. F. Gorter, Editor, North-Holland Publishing Company, Amsterdam (1955).

4. König, W., Wied. Ann. t., 43, 15 (1891).

5. Pellam, J. R., and Craig, P. P., Phys. Rev., 108, 1109 (1957).

6. Pellam, J. R., and Morse, P. M., Phys. Rev., 78, 474 (1950).

7. Pellam, J. R., in Progress in Low Temperature Physics, C. J. Gorter, Editor, North-Holland Publishing Company, Amsterdam (1955).

8. London, F., Superfluids Vol. II, John Wiley and Sons, Inc., New York, 1954.

9. Feynman, R. P., and Cohen, M., 1956, Phys. Rev., 102, 1189

10. Dingle, R. B., Advances in Physics, 1, 111 (1952).

11. Wilks, J., Reports on Progress in Physics, 20, 38 (1957).